Clustering and vacancy behavior in high- and low-solute Al–Mg–Si alloys

Sigurd Wenner[1], Katsuhiko Nishimura[2], Kenji Matsuda[2], Teiichiro Matsuzaki[3], Dai Tomono[3], Francis L. Pratt[4], Calin D. Marioara[5], and Randi Holmestad[1]

[1]Department of Physics, NTNU, Høgskoleringen 5, Trondheim NO-7491, Norway

[2]Department of Materials Science and Engineering, University of Toyama, Gofuku 3190, Toyama-shi, Toyama 930-8555, Japan

[3]Advanced Meson Science Laboratory, RIKEN Nishina Center for Accelerator Based Science, RIKEN, Wako, Saitama 351-0198, Japan

[4]ISIS Facility, Rutherford Appleton Laboratory, Chilton OX11 0QX, UK

[5]Materials and Chemistry SINTEF, Høgskoleringen 5, Trondheim NO-7491, Norway

Keywords: Al–Mg–Si alloy; precipitation; clustering; vacancies; muon spin relaxation; transmission electron microscopy

Abstract

The precipitate microstructure and vacancy distribution in Al–Mg–Si alloys with different amounts of solute and different heat treatments were investigated by transmission electron microscopy and muon spin relaxation measurements. A high amount of vacancies is normally present in Al–Mg–Si alloys as these bind to atomic clusters. We observe these vacancies to leave the material not before over-aging at very high temperatures such as 623 K, meaning that vacancies do not bind to incoherent over-aged precipitates. For samples only stored at room

temperature after solution heat treatment, a reduction of muon trapping was found at a temperature of 140 K when reducing the amount of solute in the alloy. This might be connected to a lower number density of Cluster(1), which contrary to Cluster(2) do not nucleate precipitates upon further aging of the material.

I. Introduction

Of the commercial wrought aluminium alloys, the 6*xxx* alloys, with Mg and Si as main alloying elements, have some of the most desirable properties. Their high strength, good ductility and corrosion resistance, and low processing cost make them attractive structural materials for automotive and architectural applications. This has ensured Al–Mg–Si alloys a place in condensed matter science as materials of frequent study over many decades. In particular, the strengthening phases have been well investigated. These appear as needle-shaped precipitates along $<001>_{Al}$, with lengths in the order of 10–100 nm, formed through diffusional phase transformations during heat treatment. Their metastable nature stresses the importance of aging the material at the right temperature for the right period of time to optimize the mechanical strength of an alloy. The sequence of precipitates appearing during artificial aging is commonly written [1, 2]:

SSSS → Atomic clusters → GP-zones → β''→ β' / TYPE-A/B/C (U1/U2/B′) → β / Si. (1)

The fully coherent monoclinic phase β'' [3] dominates at peak hardness, and develops into four less coherent (but still needle-shaped) phases during over-aging: The hexagonal β' [4], the

trigonal TYPE-A [5], the orthorhombic TYPE-B [5], and the hexagonal TYPE-C [5], which mostly nucleates on dislocations. The main equilibrium phase is the cubic β [5], but diamond Si may also form. Whether a particular phase forms also depends on the ratio between Mg and Si in the chemical composition of the alloy. For instance, Si-rich alloys tend to form TYPE-A, TYPE-C and Si particles during prolonged over-aging, while Mg-rich alloys gain larger fractions of β' and TYPE-B [6].

Most of the crystal structures of the phases in (1) have been solved by transmission electron microscopy (TEM) (see e.g. [6]). The powerful techniques high-resolution imaging and electron diffraction makes TEM the most applicable tool to study nano-sized precipitates in Al alloys. In addition to precipitate phases, it is important to figure out how the presence of smaller defects such as vacancies and atomic clusters vary with the aging state of the material. When embedded in an Al matrix, atomic clusters are very difficult to study using TEM, and other techniques such as 3D atom-probe tomography (APT) and differential scanning calorimetry (DSC) must be employed. Atomic clusters in Al–Mg–Si alloys have been found to come in two varieties [7, 8]: Cluster(1) and Cluster(2), with only the second one having the right composition/structure to nucleate hardening precipitates. Whether there is any order in the arrangement of the atoms in these clusters cannot be answered with current methods. Instead they are distinguished by their different formation enthalpies, growth rates, and sometimes compositions. While Cluster(1) is produced during room temperature (RT) aging, low-temperature pre-ageing (at e.g. 343–373 K) is typically required to shift the dominance in favor of Cluster(2) [7, 9]. This is however not the case for low-solute alloys, which seems to form Cluster(2) also at RT [10, 11].

Positron annihilation and muon spin techniques have also been applied to study the smallest of defects in an Al lattice [12–14]. Both positrons and muons can be interstitial defects in an Al

lattice, and move by thermally activated diffusion. In muon spin relaxation (μSR), the spin of a muon precesses in magnetic fields, even the tiny fields set up by atomic nuclei. [15] The muon then decays to a positron, which moves in the direction of the muon spin upon decay. The positron is detected outside the material, telling us how the muon spin has precessed from initial state. The speed of muon diffusion affects the spin precession rate. This enables us to find out whether any defects in the material has prevented muon diffusion ("trapped" the muon). This is measured with the muon trapping rate, how likely a muon is to be trapped by a defects per time. In a recent publication [16], we proposed an interpretation scheme for muon trapping rates in Al(–Mg)(–Si) alloys: Single substitutional atoms (Mg and Si) trap muons at low temperatures (< 100 K), while mono-vacancies trap muons at high temperatures (> 220 K). If vacancies cluster with Mg and Si atoms, their trapping peak is shifted toward lower temperatures, somewhere above 120 K in ternary Al–Mg–Si alloys. This enables the combined detection of vacancies and atomic clusters using muon spin relaxation (μSR) measurements.

In this work, we have used the previous interpretation of μSR spectra to investigate (i) a high-solute alloy close to its equilibrium condition and (ii) a low-solute alloy only stored at RT. These are two important boundary conditions, representing respectively (i) a microstructure which should be void of Mg–Si–vacancy clustering because all solute is present in equilibrium phases and (ii) a collection of clusters with a different type (Cluster(2)) than in its high-solute analog. TEM imaging was conducted on samples with considerable precipitation to gain a complete picture of their microstructure. This study addresses central questions regarding clustering and vacancy kinetics during RT storage, typical industrial aging, and over-aging, furthering our understanding of the complex precipitation process in Al–Mg–Si alloys.

II. Experimental procedure

The materials used in this study were ultrapure Al–1.6% Mg_2Si and Al–0.6% Mg_2Si (atomic fraction), cast and rolled to sheets 1 mm thick. This sheet was divided into samples of 25 mm × 25 mm before heat treatment. All samples were given a solution heat treatment (SHT) of 848 K (575 °C) for 1 hour, followed by quenching in ice water and immediate storage at RT or aging at temperatures between 373 K and 623 K.

The μSR experiments were conducted at the RIKEN-RAL Muon Facility in Oxfordshire, UK [17], using the ARGUS muon spectrometer. The muon beamline is near perfectly polarized antiparallel to the direction of muon implantation, and has a high enough intensity that about 1 million decay events in the sample are detected every minute. The sample temperature was kept constant with a helium cryostat while an adequate number of muon decay events (30–60 million) were detected per temperature point. The measured muon spin relaxation functions were compared to a database of functions simulated with the Monte Carlo technique, as described in [16, 18]. The precession of spin was simulated for muons that are freely diffusing and trapped at generic defects in the Al lattice. Temperature-dependent lattice distortions and other effects that change muon diffusion behavior are not explicitly simulated, as the diffusion and trapping rates are simply kept fixed in each simulation, with no derivations from a specific system temperature. The parameters describing the muon kinetics, in particular the muon trapping rate, were extracted from the relaxation functions measured at each sample temperature, by least-squares fitting to all simulated relaxation functions. In this work we subtract the trapping rate in pure Al from the trapping rate in the studied conditions. Although the resulting quantity is not always positive, it is a convenient way of showing the peaks relevant to substitutional defects more clearly.

TEM specimens were prepared by polishing the samples to films of thickness ≈ 100 μm, punching out 3 mm discs and electropolishing using a Struers TenuPol-5. The electrolyte consisted of 1/3 nitric acid and 2/3 methanol, and was kept at a temperature of approx. 248 K (−25 °C). Bright-field TEM images were acquired on film with a Philips CM30 operated at 150 kV. After aging or keeping the alloys at RT for a long time, the cluster/precipitate microstructure is stable, and does not change when the temperature is altered, in the range that we measure in the μSR experiments (20–300 K). What we observe in a TEM is therefore the same microstructure as what is probed in the μSR spectrometer.

III. Experimental results

We focus here on two new conditions of Al–Mg–Si alloys that represent extreme cases of solute content and heat treatment. The first condition is a 1.6% Mg2Si alloy, aged at 623 K (350 °C) for 30 minutes. This treatment was meant to produce exclusively over-aged and equilibrium phases without having a too coarse microstructure. Figure 1 shows bright-field TEM images of this material, along with images from two other samples which have been aged for 1000 minutes at lower temperatures. The precipitate phases were identified as follows: In the sample aged at 423 K (150 °C), only GP-zones and possibly small β'' are present, while the 473 K (200 °C) sample has mostly β'' and some β' needles (see also alloy A11 in [19]). The over-aged needle-shaped particles found in the sample aged at 623 K were difficult to identify as the Al matrix was etched faster than the precipitates during electropolishing, leaving most needles sticking out of the specimen surface. Judging by the aging state and the large rounded shapes of the precipitate cross-sections, only β' and TYPE-A/B/C are present [2, 6]. A few, large β particles were also found, as seen in Figure 1(d).

We measured the muon spin relaxation for the samples observed in the TEM, at temperatures from 20 K to 300 K. The muon trapping rates, subtracting the contributions from 99.99% pure Al, are shown in Figure 2. Judging by the high-temperature region (above 180 K), the sample aged at 623 K have muon kinetics most similar to binary Al–0.5% Mg, which we have included here for reference. For these two conditions, there is no trapping peak in the range 180–300 K. Such a trapping peak is a characteristic feature of the two Al–Mg–Si samples aged at lower temperatures, also shown in Figure 2.

The muon trapping rates in the second condition, an Al–0.6% Mg_2Si sample stored at room temperature for 8 days can be found in Figure 3. Two RT-stored Al–1.6% Mg_2Si conditions are included for comparison. The muon kinetics in the RT-stored low- and high-solute alloy have subtle, but clear differences, with the low-solute alloy having a closer resemblance to the kinetics in a high-solute sample aged at 473 K (included in both Figs. 2 and 3). Comparing the RT stored samples, decreasing the solute amount primarily affects the muon trapping at 20–50 K and in the dip at 140 K. At this last point, the RT-stored 0.6% Mg_2Si and 473 K aged 1.6% Mg_2Si samples even have lower trapping rates than pure Al. The relaxation functions at 140 K are shown in Figure 4.

IV. Discussion

In discussing the current results we emphasize that the focus is on understanding Al–Mg–Si alloys, their precipitation behavior and their most important lattice defects. Understanding all aspects of muon interactions with a solid, including phonon-assisted diffusion [15], trapping in the presence of thermally dependent lattice strains, and spin precession changes induced by possible magnetic fields in precipitate phases has proven a tremendous challenge. Regardless,

there is much to deduce from comparing the qualitative shapes of muon spin relaxation functions, here manifested in the muon trapping rate parameters, when coupled with previous experimental knowledge and the current TEM results.

The muon trapping rate curves in Figures 2 and 3 have two main trapping peaks separated at a temperature of approx. 120 K. In the low-temperature region, the trapping is dominated by free solute atoms, in particular Mg [9, 16]. Vacancy-free solute-rich areas such as precipitates may also affect muon kinetics at low temperature, but we have not observed any compelling evidence for this. In the high-temperature region, vacancies are responsible for the trapping [16], and since vacancies form strong bonds with Si and Mg in Al, they will in most cases be found in connection with atomic clusters or GP-zones [20]. When an alloy microstructure evolves during aging, we reach a point where the high-temperature muon trapping, and thus vacancy content, starts to decrease.

A 1.6% Mg_2Si sample aged at 473 K has a lower muon trapping than one aged at 423 K, and after merely 30 minutes of aging at 623 K, the trapping is close to absent when measuring above 120 K (see Figure 2). The remaining trapping might be caused by free vacancies. The coarse microstructure of the high-temperature aged sample [Figure 1(c–d)] does not contain any precipitates that are fully coherent with the Al matrix (such as β''), while these are abundant in the 473 K aged sample. Evidently, over-aged incoherent precipitates do not trap vacancies, although vacancies may be annihilated at the precipitate–matrix interface. This was also observed for the Si phase in Al [16]. The ability of coherent clusters (an maybe precipitate phases) to trap vacancies is an important factor in precipitation kinetics, as this limits the diffusion rate of solute atoms during clustering [20].

The most prominent difference in muon trapping amongst high- and low-solute alloys happens at a temperature of 140 K. Figure 4 shows the muon spin relaxation functions at this point, and it is clear from these that the RT stored high-solute alloys have a significantly higher spin relaxation rate than the two other conditions. This is caused by muons being localized at defects rather than diffusing [15]. The difference can not simply be attributed to a change in cluster number density or size. This because the trapping rate curves for Al–1.6% Mg_2Si RT stored for two weeks and half a year are almost indistinguishable, although their clustering states are quite distinct, seen e.g. in the strong RT hardness evolution [21]. The structure of the clusters is assumed to be an essential factor for the shape of the trapping rate curve. Judging by the reduced muon trapping at the temperature 140 K, the RT stored Al–0.6% Mg_2Si sample should therefore contain clusters with a structure similar to that in Al–1.6% Mg_2Si aged at 473 K. One possibility is that Cluster(1), introduced in Section I, is the cause of the trapping around 140 K. In the low-solute alloy, all the solute might exclusively go into forming Cluster(2), while annealing at 473 K have dissolved all Cluster(1) in the high-solute alloy. Other than this, we see no obvious distinction between different cluster types based on the data obtained by μSR.

Being pure and without grain refiners, the investigated alloys have large grain sizes (~ 100 μm). Though pure Al has undergone the same process route, it contains subgrains of a size ~ 1 μm, which are not seen in any of the alloys. This may be the reason behind the broad trapping peak from 50 K to 220 K in pure Al (see Figure 2). No difference in grain size was found in the alloys, and subgrain growth does not occur during aging at 200 K. The effects of polycrystallinity should therefore not give any differences among the muon trapping rates in the alloys. It can however explain the negative values of muon trapping rate around 140 K in some

alloys: Subgrain boundaries may add muon trapping centers in pure Al, while no defects affect muon diffusion in the alloys at this point, unless Cluster(1) is present.

V. Conclusion

We have investigated the micro- and nanostructures in Al–Mg–Si alloys with heat treatments designed for probing the vacancy and clustering kinetics during artificial aging. We employed μSR for detecting vacancies and atomic clusters, while TEM was used to provide an overview of the precipitate microstructure in the samples. The following conclusions can be drawn:

- With μSR measurements, we have strengthened the hypothesis of [12]: That Mg–Si clusters trap vacancies and keep them inside the material during aging, while incoherent precipitates such as TYPE-A/B/C, Si and β do not trap vacancies.
- We compared the muon kinetics in low-solute (Al–0.6% Mg_2Si) and high-solute (Al–1.6% Mg_2Si) alloys stored at room temperature. At a measurement temperature of 140 K, the muon trapping is lower in the high-solute alloy. Trapping at this peak may be associated with Cluster(1): If the solute in an alloy is sparse, it all goes into the more beneficial Cluster(2) instead.

This work has led to a more complete picture of the kinetics of vacancies and clustering during room temperature storage and aging of Al–Mg–Si alloys.

Acknowledgements

This work was financially supported by The Research Council of Norway and Norsk Hydro via project no. 193619, The Norwegian–Japanese Al–Mg–Si Alloy Precipitation Project.

References

[1] G.A. Edwards, K. Stiller, G.L. Dunlop and M.J. Couper: *Acta Mater.*, 1998, vol. 46, pp. 3893–3904.

[2] K. Matsuda, Y. Sakaguchi, Y. Miyata, Y. Uetani, T. Sato, A. Kamio and S. Ikeno: *J. Mater.Sci.*, 2000, vol. 35, pp. 179–189.

[3] H.W. Zandbergen, S.J. Andersen, and J. Jansen, *Science*, 1997, vol. 277, pp. 1221–1225.

[4] R. Vissers, M.A. van Huis, J. Jansen, H.W. Zandbergen, C.D. Marioara, S.J. Andersen, *Acta Mater.*, 2007, vol. 55, pp. 3815–3823.

[5] C. Ravi and C. Wolverton, *Acta Mater.*, 2004, vol. 52, pp. 4213–4227.

[6] C.D. Marioara, H. Nordmark, S.J. Andersen and R. Holmestad: *J. Mater. Sci.*, 2006, vol. 41, pp. 471–478.

[7] A. Serizawa, S. Hirosawa and T. Sato: *Metall. Mater. Trans. A*, 2008, vol. 39, pp. 243–251.

[8] S. Kim, J. Kim, H. Tezuka, E. Kobayashi and T. Sato: *Mater. Trans.*, 2013, vol. 54, pp. 297–303.

[9] F. De Geuser, W. Lefebvre and D. Blavette: *Phil. Mag. Lett.*, 2006, vol. 86, 227–234.

[10] C.S.T. Chang, I. Wieler, N. Wanderka and J. Banhart: *Ultramicroscopy*, 2009, vol. 109, pp. 585–592.

[11] F.A. Martinsen, F.J.H. Ehlers, M. Torsæter and R. Holmestad: *Acta Mater.*, 2012, vol. 60, pp. 6091–6101.

[12] M, Doyama. T. Hatano, T. Natsui, Y. Suzuki, Y.J. Uemura, T. Yamazaki, J.H. Brewer and K. Crowe: *Hyperfine Interact.*, 1984, vol. 17, pp. 225–229.

[13] A. Dupasquier, G. Kögel and A. Somoza: *Acta mater.*, 2004, vol. 52, pp. 4707–4726.

[14] J. Banhart, M.D.H. Lay, C.S.T. Chang and A.J. Hill: *Phys. Rev. B*, 2011, vol. 83, pp. 014101.

[15] A.Yaouanc and P.D. de Réotier: *Muon Spin Rotation, Relaxation, and Resonance: Applications to Condensed Matter*, p. 115, Oxford University Press, Oxford, 2011.

[16] S. Wenner, K. Nishimura, K. Matsuda, T. Matsuzaki, D. Tomono, F.L. Pratt, C.D. Marioara and R. Holmestad: *Acta mater.*, 2013, vol. 61, pp. 6082–6092.

[17] T. Matsuzaki, K. Ishida, K. Nagamine, I. Watanabe, G.H. Eaton and W.G. Williams: *Nucl. Instr. Methods A*, 2001, vol. 465, pp. 365–383.

[18] S. Wenner, R. Holmestad, K. Matsuda, K. Nishimura, T. Matsuzaki, D. Tomono, F.L. Pratt and C.D. Marioara: *Phys. Rev. B.*, 2012, vol. 86, pp. 104201.

[19] C.D. Marioara, S.J. Andersen, H.W. Zandbergen and R. Holmestad: *Metall. Mater. Trans. A*, 2005, vol. 36, pp. 691–702.

[20] H.S. Zurob and H. Seyedrezai, *Scripta Mater.*, 2009, vol. 61, pp. 141–144.

[21] S. Wenner, C.D. Marioara, S.J. Andersen and R. Holmestad: *Int. J. Mater. Res.*, 2012, vol. 103, pp. 948–954.

Figures

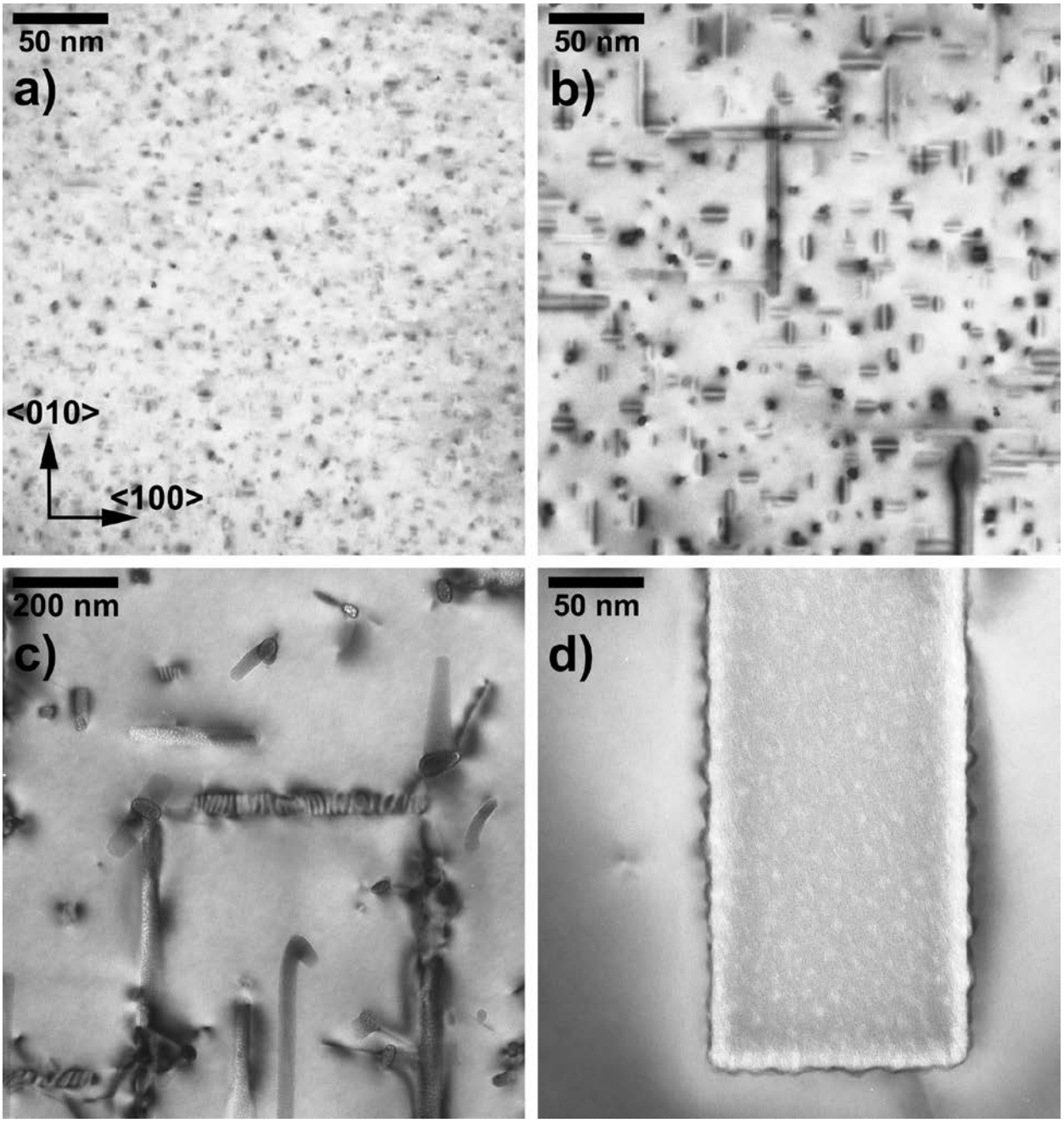

Figure 1: Bright-field TEM images of precipitate microstructures in 1.6% Mg_2Si, viewed along $<001>_{Al}$. (a) Material aged for 1000 min at 423 K. (b) Aged for 1000 min at 473 K. (c–d) Aged for 30 min at 623 K.

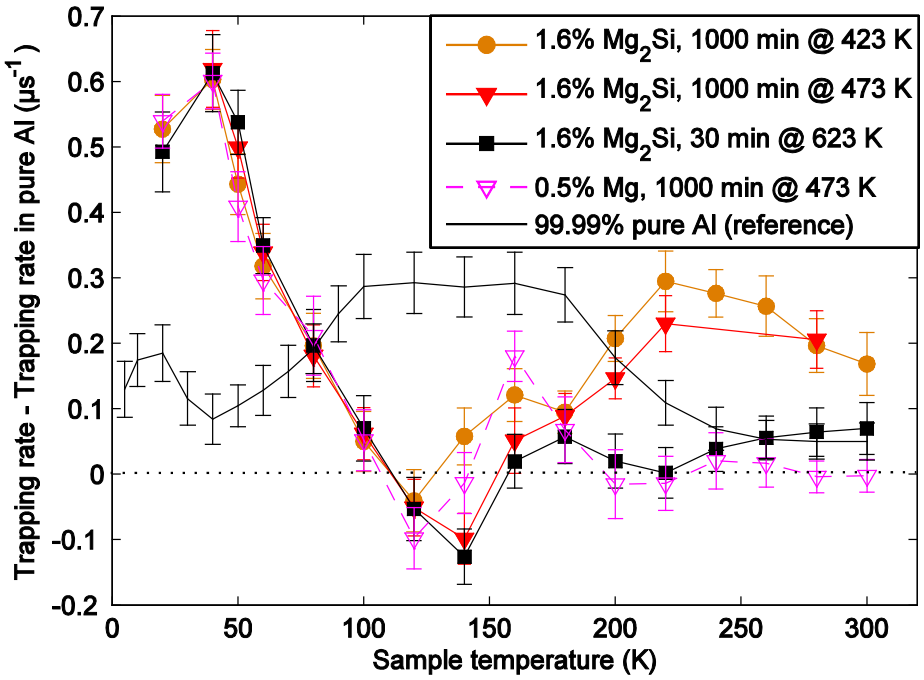

Figure 2: Muon trapping rate in aged Al–Mg–Si alloys. The pure Al reference curve is subtracted from the others. Al–0.5% Mg is included as it has the behavior most similar to that of 1.6% Mg_2Si aged at 623 K.

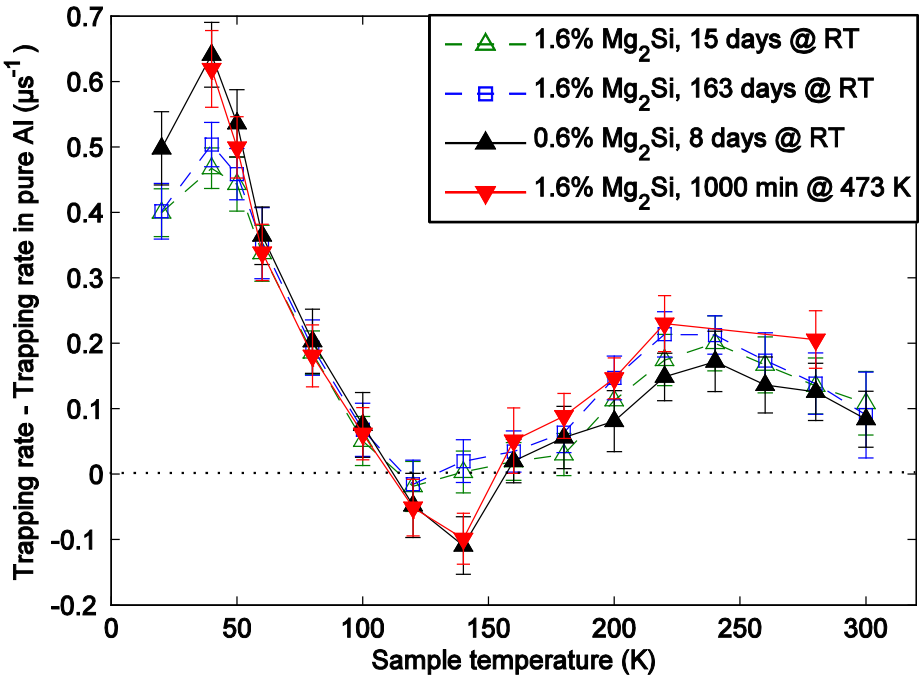

Figure 3: Muon trapping rate in Al–Mg–Si alloys stored at room temperature (RT) after solution heat treatment. The pure Al reference curve (see Figure 2) is subtracted from the others. Al–1.6% Mg_2Si is included as it has the behavior most similar to that of 0.6% Mg_2Si stored at RT.

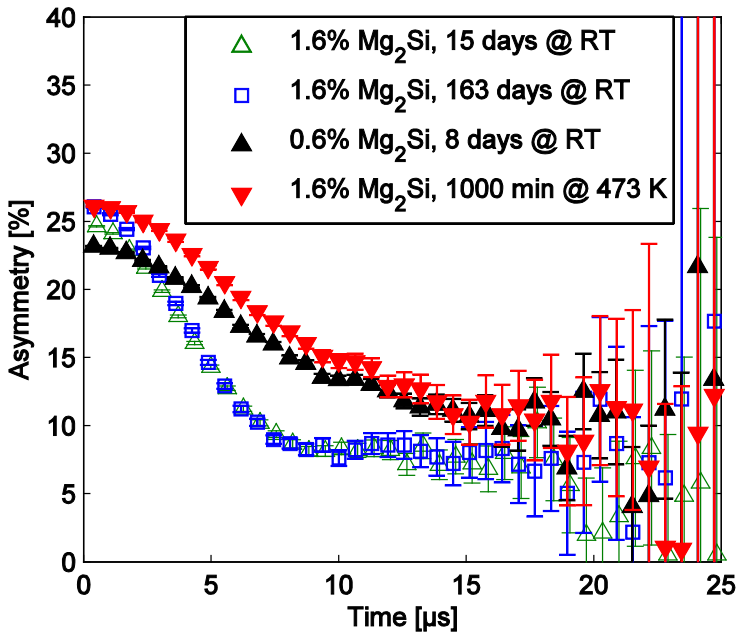

Figure 4: Muon spin relaxation functions of the conditions in Figure 3, at a sample temperature of 140 K. The lower initial asymmetry of the Al–0.6% Mg_2Si sample is caused by slightly different experimental conditions.